

## Brequinar derivatives and species-specific drug design for dihydroorotate dehydrogenase<sup>☆</sup>

Darrell E. Hurt,<sup>a</sup> Amanda E. Sutton<sup>a</sup> and Jon Clardy<sup>b,\*</sup>

<sup>a</sup>Department of Chemistry and Chemical Biology, Cornell University, Ithaca, NY 14850, USA

<sup>b</sup>Department of Biological Chemistry and Molecular Pharmacology, Harvard Medical School, Boston, MA 02115, USA

Received 15 September 2005; revised 7 December 2005; accepted 7 December 2005

Available online 10 January 2006

**Abstract**—Therapeutic agents brequinar sodium and leflunomide (Arava<sup>TM</sup>) work by binding in a hydrophobic tunnel formed by a highly variable N-terminus of family 2 dihydroorotate dehydrogenase (DHODH). The X-ray crystallographic structure of an analog of brequinar bound to human DHODH was determined. In silico screening of a library of compounds suggested another subset of brequinar analogs that do not inhibit human DHODH as potentially effective inhibitors of *Plasmodium falciparum* DHODH. © 2005 Elsevier Ltd. All rights reserved.

Inhibition of dihydroorotate dehydrogenase (DHODH) is the target of several drugs developed to treat cancer, transplant rejection, rheumatoid arthritis, psoriasis, and autoimmune diseases.<sup>1</sup> DHODH inhibitors have also been suggested as antibiotics,<sup>2</sup> especially against *Helicobacter pylori*,<sup>3</sup> and as antifungal agents.<sup>4</sup> These inhibitors act by abrogating the rate-limiting step of de novo pyrimidine biosynthesis. In this reaction, dihydroorotate is oxidized to orotate through a flavin prosthetic group that couples dihydroorotate oxidation to respiratory quinone reduction. Orotate is a precursor to uridine monophosphate, the base from which all other pyrimidines are manufactured in the cell. Pyrimidines are critical elements in DNA, RNA, various cofactors, protein glycosylation, membrane lipid biosynthesis, and strand break repair.<sup>5</sup>

The exclusive use of respiratory quinones as an electron sink distinguishes the mostly eukaryotic family 2 from the mostly prokaryotic family 1 DHODH.<sup>6</sup> Structural

studies<sup>7–11</sup> confirm that an N-terminal domain found only in family 2 DHODH provides the membrane association required to use quinones.<sup>11–13</sup> Two  $\alpha$ -helices in the N-terminal domain provide a distinct binding site for quinones. The quinone-binding site is preceded in eukaryotic organisms by a single membrane-anchoring transmembrane helix and a mitochondrial signaling sequence.<sup>14,15</sup> Truncation of these elements does not impact in vitro activity<sup>16,17</sup> although it does result in the loss of in vivo activity due to improper cellular localization.<sup>18,19</sup>

Many inhibitors of family 2 DHODH bind in the quinone-binding site.<sup>7–11</sup> Certain compounds inhibit DHODH from one species much more than others.<sup>2,4,20–23</sup> The low measure of sequence similarity between species in the N-terminal domain is thought to contribute this high degree of species-related preferential inhibition. As part of a larger program to develop novel inhibitors specific to *Plasmodium falciparum* DHODH (PfDHODH), a series of compounds was synthesized in an attempt to exploit these sequence differences.<sup>24</sup> Although these compounds performed poorly as inhibitors of PfDHODH, a crystallographic analysis of one of these compounds bound to human DHODH (HsDHODH) was undertaken as a proof of concept. With the recent appearance of new structures of DHODH in public databases, in silico screening provides a way to probe these structures for subtle differences that may account for the observed species-related preferential inhibition and suggest new directions for inhibitor design and screening.

**Abbreviations:** DHODH, dihydroorotate dehydrogenase; FMN, flavin mononucleotide; HsDHODH, *Homo sapiens* DHODH; PfDHODH, *Plasmodium falciparum* DHODH; RrDHODH, *Rattus rattus* DHODH; C<sub>8</sub>E<sub>5</sub>, pentaethylene glycol mono-octyl ether; DCIP, 2,6-dichloroindophenol; DCL, dichloroallyl lawsone.

**Keywords:** Drug design; Dihydroorotate dehydrogenase; Brequinar.

<sup>☆</sup> The atomic coordinates have been deposited in the Protein Data Bank, [www.rcsb.org](http://www.rcsb.org) (PDB ID code: 2B0M).

\* Corresponding author. Tel.: +301 594 9225; fax: +301 480 2282; e-mail: [jon-clardy@hms.harvard.edu](mailto:jon-clardy@hms.harvard.edu)

The synthesis of the brequinar-derived asymmetric terphenyl compounds (Fig. 1 and Table 1) is discussed elsewhere.<sup>24</sup> Their design is a hybrid of the scaffold of brequinar and binding motifs from another well-known DHODH inhibitor, A77 1726.

For each of these compounds, a crude visual assay based on the color change in the dye 2,6-dichloroindophenol (DCIP,  $\epsilon_{595} = 18.8 \text{ mM}^{-1} \text{ cm}^{-1}$ ) was used to first establish a threshold concentration required for inhibition.<sup>17</sup> Compounds that were effective below 100  $\mu\text{M}$  were subjected to a more quantitative assay to determine their inhibition constant. In each kind of assay, the concentration of dihydroorotate remained fixed at a saturating level (250  $\mu\text{M}$ ). The electron receptor used was 2,3-dimethoxy-5-methyl-6-(3-methyl-2-butenyl)-1,4-benzoquinone ( $\text{CoQ}_1$ ). Kinetic parameters were determined by varying the concentration of  $\text{CoQ}_1$  (25–100  $\mu\text{M}$ ). Competitive inhibition assays varied the concentration of both inhibitor (15–60  $\mu\text{M}$ ) and  $\text{CoQ}_1$  (25–100  $\mu\text{M}$ ). Reactions were initiated by the addition of purified enzyme to a final concentration of 20 nM.

Values for the Michaelis–Menten constant ( $K_m = 6.6 \pm 0.7 \mu\text{M}$ ), the catalytic rate ( $k_{\text{cat}} = 15.4 \pm 0.2 \text{ s}^{-1}$ ), and the specificity constant ( $k_{\text{cat}}/K_m = 2.3 \pm 0.2 \text{ s}^{-1} \mu\text{M}^{-1}$ ) are slightly different from published values for HsDHODH,<sup>17,25</sup> but the quinone substrate used in our experiments is different than the ones used in previous studies. The results of the inhibition assays are shown in Table 1.

Expression, purification, and crystallization of HsDHODH were performed using the published procedure.<sup>9</sup> Compound AMX02 was co-crystallized with HsDHODH in place of brequinar. Crystals grown under sitting drop vapor diffusion belonged to space group

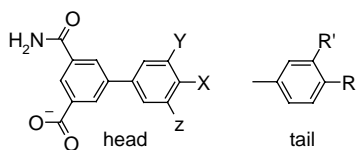


Figure 1. Brequinar-derived asymmetric terphenyl compounds.

Table 1. HsDHODH inhibition constants for designed inhibitors

Compound	Tail	Substituents	$R'$	$K_i^C$ ( $\mu\text{M}$ )	$K_i^U$ <sup>a</sup> ( $\mu\text{M}$ )
AMX02	X	R = H,	R' = H	$2.8 \pm 0.4$	
AMX07	Y	R = CH <sub>3</sub> ,	R' = H	$4 \pm 3$	
AMX06	Y	R = H,	R' = H	$20 \pm 3$	
AMX08	Y	R = H,	R' = CH <sub>3</sub>	$3.7 \pm 0.9$	$50 \pm 10$
AMX01	Y	R = C(CH <sub>3</sub> ) <sub>3</sub> ,	R' = H	$4 \pm 1$	$90 \pm 20$
AMX10	Y	R = CF <sub>3</sub> ,	R' = H	$6 \pm 2$	$90 \pm 30$
AMX04	X	R = CF <sub>3</sub> ,	R' = H	>100,000	
AMX05	X	R = C(CH <sub>3</sub> ) <sub>3</sub> ,	R' = H	>100,000	
AMX03	X	R = CH <sub>3</sub> ,	R' = H	>100,000	
AMX09	Y,Z	R = H,	R' = H	>100,000	

<sup>a</sup> All compounds displayed competitive inhibition, except for those for which a  $K_i^U$  is reported; these displayed mixed inhibition. Errors are the standard error for the fit.

$P3_221$ , with  $a = b = 90.4 \text{ \AA}$  and  $c = 123.3 \text{ \AA}$ . Data were collected at 100 K on the F2 beamline at the Cornell High Energy Synchrotron Source (CHESS) with an ADS Quantum 4 CCD detector. All data were reduced with HKL2000<sup>26</sup> (Table 2). Molecular replacement with MolRep<sup>27</sup> using only the protein portion of HsDHODH (PDB ID: 1D3G) as a search model provided the solution to the phase problem. Difference maps ( $F_O - F_C$ ) displayed well-defined density for the hetero-compounds before building them into the molecular model with O.<sup>28,29</sup> Refinement of the model with CNS<sup>30</sup> (Table 2) using parameters from the Hetero-compound Information Centre–Uppsala<sup>31</sup> for the substrates and prosthetic group yielded a satisfactory model. Molecular graphics were prepared with SPOCK,<sup>32</sup> MolScript,<sup>33</sup> POV-Script+,<sup>34</sup> and POV-Ray.<sup>35</sup>

This structure of HsDHODH is nearly identical (0.3  $\text{\AA}$  backbone rms displacement) to previous structures of HsDHODH.<sup>9</sup> Eight parallel  $\beta$ -strands form the inner core of a canonical  $\alpha/\beta$  barrel. Eight  $\alpha$ -helices flank these  $\beta$ -strands and form the outer shell of the barrel. Two short anti-parallel  $\beta$ -strands lie flat on the N-terminal ends of the inner  $\beta$ -barrel. A flavin mononucleotide (FMN) prosthetic group sits in the other end of the

Table 2. Diffraction and refinement statistics<sup>a</sup>

Beamline	CHESS F2
Wavelength ( $\text{\AA}$ )	0.9793
Oscillation ( $\phi$ , $^\circ$ )	1
Exposure (s)	20–30
Resolution	$50 > d > 2.0$
Reflections, total	209,728
Reflections, unique	37,871
Completeness (%)	94.7 (86.1)
$\langle I/\sigma(I) \rangle$	11.7 (8.4)
Multiplicity	5.5 (2.4)
$R_{\text{sym}}$ (%)	10.9 (37.0)
Unit cell	$P3_221$ $a = b = 90.4 \text{ \AA}$ $c = 123.3 \text{ \AA}$
Refinement reflections, total	37,631
Work	35,765 (3241)
Test	1866 (156)
Completeness (%)	89.4 (81.8)
Atoms, total	2964
Protein	2757
Ligands	66
Water	141
$R$ (%)	21.8 (25.0)
$R_{\text{free}}$ (%)	25.0 (29.0)
Luzzati plot/cross-validated	0.24/0.28
SIGMAA/cross-validated	0.16/0.16
Rms bond length ( $\text{\AA}$ )/angle ( $^\circ$ )	0.007/1.22
Rms dihedral ( $^\circ$ )/improper ( $^\circ$ )	21.4/0.81
Rms B bonds ( $\text{\AA}^2$ )/angles ( $\text{\AA}^2$ )	
Main chain	1.22/1.82
Side chain	2.06/3.03
Ramachandran plot	
Most favored (%)	91.3
Additionally allowed (%)	8.0
Generously allowed (%)	0.3
Disallowed (%)	0.3

<sup>a</sup> Highest resolution shell values in parentheses.

barrel and is held in place by a protruding sheet of anti-parallel  $\beta$ -strands. A flexible loop near these  $\beta$ -strands opens to reveal the dihydroorotate-binding site. On the outside of the barrel, near these  $\beta$ -strands, two  $\alpha$ -helices of the N-terminal domain form the quinone-binding site. These  $\alpha$ -helices are loosely tethered to the N-terminal end of the barrel domain by a poorly defined loop of 15 residues. As previously observed, the presence of some kind of inhibitor in the quinone-binding site was required for crystallization, suggesting that the ligand stabilizes and minimizes the motion of the N-terminal  $\alpha$ -helices. Short  $3_{10}$  helices were identified using DSSP<sup>36</sup> and STRIDE<sup>37</sup> at the C-terminus and at junctions between some of the  $\beta$ -strands and  $\alpha$ -helices.

Oxidized orotate and FMN were modeled into the well-defined electron density describing the dihydroorotate- and FMN-binding sites. The presence of the two oxidized species probably represents the trapping of an air-oxidized species in the crystalline environment because such a configuration is not physiologically relevant.<sup>38</sup> As with the structure of HsDHODH bound to brequinar, unmistakable electron density marks the presence of an amine- $\beta$ -oxide detergent molecule in the mouth of the quinone-binding tunnel.

As expected, the terphenyl compound AMX02 binds in the quinone-binding site in a fashion similar to brequinar (Fig. 2). The phenyl tail is held in the tunnel by hydrophobic interactions. The carboxylic acid moiety hydrogen bonds with R136 and the amide group hydrogen bonds to Y356 near the FMN group. The lack of hydrophobic contacts near V134 and V143 may be one

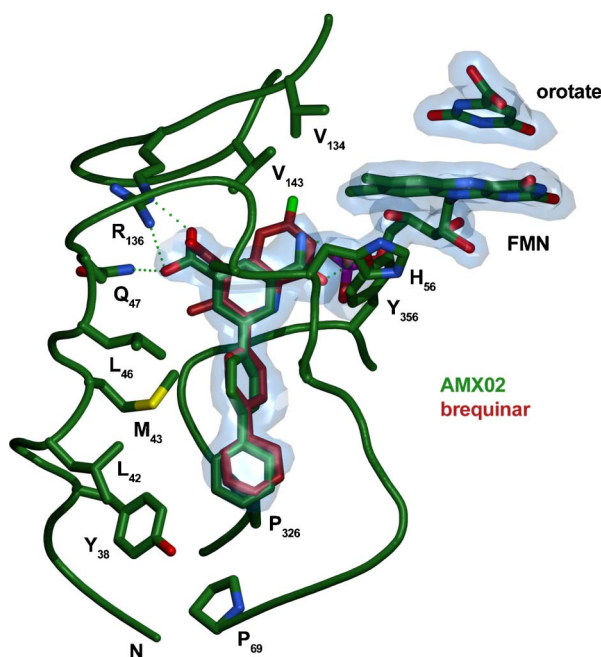


**Figure 2.** The binding pocket of HsDHODH with AMX02 bound (forest). Hydrogen bonds to R136, Q47, and Y356 are similar to hydrogen bonding with brequinar (firebrick). Electron density (marine) for AMX02, FMN, and orotate is shown at  $1\sigma$ .

reason for the decreased affinity of HsDHODH for this compound as compared to brequinar.

Many measurements have already been made of the inhibition of HsDHODH by several compounds, including A77 1726,<sup>16,20,38,39</sup> brequinar<sup>20,21,38–46</sup>, and atovaquone.<sup>43,46,47</sup> Similar measurements have been made for rat DHODH (RrDHODH) with A77 1726<sup>48</sup>, brequinar,<sup>20,43,48</sup> and atovaquone.<sup>43,46</sup> Other inhibitors have been tested as well.<sup>16,22,49–54</sup> Several quantitative structure–activity relationship studies have also been made.<sup>20,41,55–59</sup> Some preference is observed between mammalian DHODHs. Brequinar inhibits HsDHODH about 40 times more potently than RrDHODH, but A77 1726 inhibits RrDHODH about 60 times more potently than HsDHODH.<sup>20</sup> A greater degree of preferential inhibition exists between more distantly related species. Brequinar is a potent inhibitor of mammalian DHODH, but it does not inhibit *P. falciparum*, *Escherichia coli*,<sup>21</sup> or *Arabidopsis thaliana*<sup>22</sup> membrane-associated DHODH. A series of A77 1726 analogs inhibit HsDHODH 2000–5700 times more potently than PfDHODH.<sup>23</sup> The series of asymmetric terphenyl compounds inhibit HsDHODH, but not PfDHODH. Other examples of inhibitors that display species-related preference among membrane-associated DHODHs include a series of substituted thiadiazolidinediones that inhibit *E. coli* and *Enterobacter faecalis*, but not human, DHODH,<sup>2</sup> and an agricultural antifungal, LY214352, that inhibits *Aspergillus nidulans*, but not *E. coli*, DHODH.<sup>4</sup> Finally, redoxal and dichloroallyl lawsone (DCL) inhibit mammalian DHODH, but not PfDHODH.<sup>23</sup>

The variable nature of the quinone-binding tunnel is thought to be responsible for the species-related preferential inhibition for compounds that bind in the tunnel. All of the compounds described above have known inhibition constants for DHODH, although not all of them are potent inhibitors. Docking a database of compounds of known potency to the known structures of membrane-associated DHODH is one method to probe the structural details that influence specificity for inhibitors in different species. If a set of compounds docks well with the enzyme from one species and poorly with another, then that set helps describe the specificity.

A three-dimensional geometry-optimized model for each compound described in previous studies was generated from two-dimensional sketches or SMILES strings. Multiple conformations and atomic point charges were assigned using tools provided with ZINC.<sup>60</sup> This database was docked to the quinone-binding site of human (PDB ID: 1D3G), rat (PDB ID: 1UUM, 1UOO), and *P. falciparum* (PDB ID: 1TV5) DHODH by the computer package eHiTS<sup>®</sup> using default parameters.<sup>61</sup> Although there are now three structures of HsDHODH bound to an inhibitor, only one structure was selected for docking because in each structure, the inhibitor lies in nearly the same place and defines the binding site. Two structures of rat DHODH (RrDHODH) were selected because inhibitor binding has a more pronounced effect upon the structure of the quinone-binding tunnel, leading to structural differences to be probed by docking.

The eHiTS<sup>®</sup> package uses a systematic algorithm to generate all compatible docking modes to cover the entire docking space and ensure a complete solution. This process avoids the arbitrary subset of possible solutions inherent in sampling methods. The docking algorithm is divided into an exhaustive search algorithm based on graph matching and a novel scoring function based on local surface point contact evaluation.

The exhaustive search is made by splitting up the ligand into flexible and rigid fragments, and then fitting them into every possible region of the receptor site. These fragments are then combined to form a graph where the nodes are the fragments and the edges are the connecting chains. The graph of the receptor site has nodes for pockets where ligand fragments can be placed and edges that represent distances between the pockets. The graphs are matched by applying flexible ligand chains to reconnect the rigid fragments. Finally, each reconstituted ligand pose is subjected to local energy minimization. In this way, every possible conformation and orientation will be evaluated.

The evaluation of poses depends on a fine grid based on the surface of the receptor site that has information on the chemical and atomic properties that make up that surface. Some properties that are considered include hydrogen bonding, hydrophobicity, electrostatic potential, van der Waals contact energy, ionic interactions, and pocket depth (considers changes in the dielectric constant). Each point on the grid is assigned a score based on its interaction with each atom of the ligand that is within a threshold distance. Points that have no ligand atom within the cutoff distance are assigned a penalty score. The sum of point scores constitutes the score for that pose of the ligand. By default, the lowest scoring pose for a given ligand is reported. The score is not an absolute measure of the binding energy, but differences in score for a given receptor site can be loosely compared in terms of energy (kcal/mol).

The measure of the effectiveness ( $E_{\text{diff}}$ ) of a compound as a potential inhibitor for a particular enzyme was calculated by subtracting the score for that compound from the score of the best scoring compound of the entire set of ligands for that enzyme. Ligands with small values for  $E_{\text{diff}}$  are much more likely to bind and be good inhibitors than ligands with greater  $E_{\text{diff}}$  values.

Docking with eHiTS<sup>®</sup> produced trends in scores that were largely in agreement with experimentally determined measures of inhibition, especially for atovaquone and brequinar. The rms deviation in position for these docked compounds as compared to their crystal structures was less than 0.5 Å. This agreement permits a degree of confidence in the predictions of the docking algorithm.

As expected, most analogs of brequinar and a novel set of compounds<sup>55</sup> dock well to human and rat DHODH. Also as expected, some analogs of brequinar<sup>57</sup> known to not inhibit HsDHODH ( $IC_{50} > 10 \mu\text{M}$ ) did not dock well to human or rat DHODH ( $E_{\text{diff}} > 12.5$ ). However,

these same poor inhibitors of HsDHODH scored well ( $E_{\text{diff}} = 0, 0.57, \text{ and } 1.17$ ) when docked to PfDHODH (Fig. 3). These compounds are similar to those predicted<sup>7</sup> and those recently found through high-throughput screening<sup>62</sup> as PfDHODH inhibitors. In addition to these compounds, a thiadiazolidione that inhibits bacterial DHODH but is known to be a poor inhibitor of HsDHODH ( $IC_{50} > 100 \mu\text{M}$ )<sup>2</sup> scored poorly when docked to HsDHODH, but scored well when docked to PfDHODH.

Our series of asymmetric terphenyl compounds was designed to avoid the larger side chains ( $I_{\text{Pr}263}$  and  $I_{\text{Pr}272}$ ) of the hydrophobic residues found near the FMN of the PfDHODH quinone-binding tunnel. The compounds successfully avoid clashes with those side chains, but, like brequinar, are deficient in other ways. The large side chain of  $F_{\text{Pr}188}$  occupies the same position as the tail of brequinar in HsDHODH and RrDHODH (and AMX02 in HsDHODH), suggesting a reason why brequinar and the series of terphenyl compounds are not effective inhibitors of PfDHODH.<sup>7</sup> The subset of brequinar analogs and the thiadiazolidione identified by in silico screening may be effective inhibitors of PfDHODH because they avoid this steric clash (Fig. 3).

This study provides another structure of a family 2 DHODH and suggests a subset of brequinar analogs known to be poor inhibitors of HsDHODH as potentially high-affinity inhibitors of PfDHODH. Existing libraries of brequinar compounds should therefore be

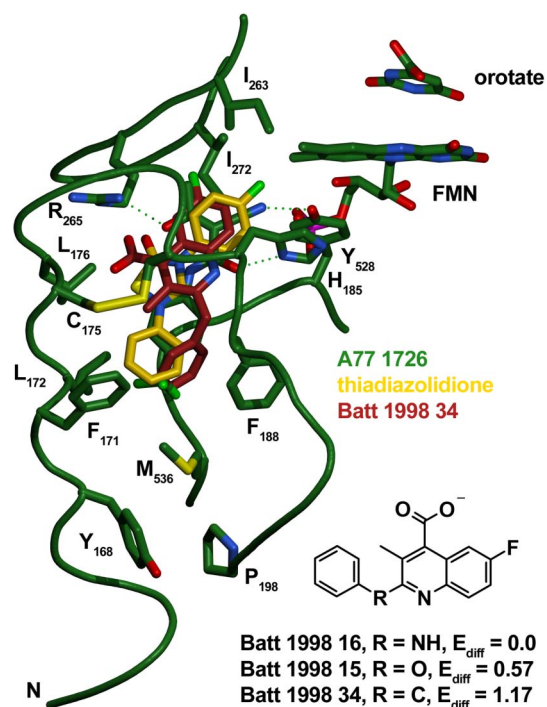


**Figure 3.** The binding pocket of PfDHODH with A77 1726 bound (forest). Batt 1998 34 (firebrick) and a thiadiazolidione (gold) were identified as possible inhibitors specific to PfDHODH. They reside in the same place in the binding pocket as does A77 1726 and avoid clashing with  $F_{\text{Pr}188}$ , the major obstacle to brequinar and AMX02 binding in PfDHODH.

screened as inhibitors of PfDHODH. Novel chemotypes have recently been discovered as inhibitors of HsDHODH and should be explored as PfDHODH inhibitors as well.<sup>55,62,63</sup> The broad spectrum of potential applications for DHODH inhibitors as therapeutic agents against infectious and autoimmune diseases should stimulate further development of potent and species-specific DHODH inhibitors.

### Acknowledgment

The authors thank NIH CA59021 and the Burroughs Wellcome Fund for their generous support.

### References and notes

- Kovarik, J. M.; Burtin, P. *Expert Opin. Emerg. Drugs* **2003**, *8*, 47.
- Marcinkeviciene, J.; Rogers, M. J.; Kopcho, L.; Jiang, W.; Wang, K.; Murphy, D. J.; Lippy, J.; Link, S.; Chung, T. D.; Hobbs, F.; Haque, T.; Trainor, G. L.; Slee, A.; Stern, A. M.; Copeland, R. A. *Biochem. Pharmacol.* **2000**, *60*, 339.
- Copeland, R. A.; Marcinkeviciene, J.; Haque, T. S.; Kopcho, L. M.; Jiang, W.; Wang, K.; Ecret, L. D.; Sizemore, C.; Amsler, K. A.; Foster, L.; Tadesse, S.; Combs, A. P.; Stern, A. M.; Trainor, G. L.; Slee, A.; Rogers, M. J.; Hobbs, F. *J. Biol. Chem.* **2000**, *275*, 33373.
- Gustafson, G.; Davis, G.; Waldron, C.; Smith, A.; Henry, M. *Curr. Genet.* **1996**, *30*, 159.
- Löffler, M.; Jockel, J.; Schuster, G.; Becker, C. *Mol. Cell. Biochem.* **1997**, *174*, 125.
- Nagy, M.; Lacroute, F.; Thomas, D. *Proc. Natl. Acad. Sci. U.S.A.* **1992**, *89*, 8966.
- Hurt, D. E.; Widom, J.; Clardy, J. *Acta Crystallogr. D Biol. Crystallogr.* **2005**.
- Rowland, P.; Nielsen, F. S.; Jensen, K. F.; Larsen, S. *Structure* **1997**, *5*, 239.
- Liu, S.; Neidhardt, E. A.; Grossman, T. H.; Ocain, T.; Clardy, J. *Struct. Fold Des.* **2000**, *8*, 25.
- Nørager, S.; Jensen, K. F.; Björnberg, O.; Larsen, S. *Structure* **2002**, *10*, 1211.
- Hansen, M.; Le Nours, J.; Johansson, E.; Antal, T.; Ullrich, A.; Löffler, M.; Larsen, S. *Protein Sci.* **2004**, *13*, 1031.
- Jensen, K. F.; Björnberg, O. *Paths Pyrimidines* **1998**, *6*, 20.
- Björnberg, O.; Rowland, P.; Larsen, S.; Jensen, K. F. *Biochemistry* **1997**, *36*, 16197.
- Krogh, A.; Larsson, B.; von Heijne, G.; Sonnhammer, E. L. L. *J. Mol. Biol.* **2001**, *305*, 567.
- Moller, S.; Croning, M. D. R.; Apweiler, R. *Bioinformatics* **2001**, *17*, 646.
- Davis, J. P.; Cain, G. A.; Pitts, W. J.; Magolda, R. L.; Copeland, R. A. *Biochemistry* **1996**, *35*, 1270.
- Copeland, R. A.; Davis, J. P.; Dowling, R. L.; Lombardo, D.; Murphy, K. B.; Patterson, T. A. *Arch. Biochem. Biophys.* **1995**, *323*, 79.
- Löffler, M.; Knecht, W.; Rawls, J.; Ullrich, A.; Dietz, C. *Insect Biochem. Mol. Biol.* **2002**, *32*, 1159.
- Rawls, J.; Knecht, W.; Diekert, K.; Lill, R.; Löffler, M. *Eur. J. Biochem.* **2000**, *267*, 2079.
- Knecht, W.; Löffler, M. *Biochem. Pharmacol.* **1998**, *56*, 1259.
- Chen, S. F.; Perrella, F. W.; Behrens, D. L.; Papp, L. M. *Cancer Res.* **1992**, *52*, 3521.
- Ullrich, A.; Knecht, W.; Piskur, J.; Löffler, M. *FEBS Lett.* **2002**, *529*, 346.
- Baldwin, J.; Farajallah, A. M.; Malmquist, N. A.; Rathod, P. K.; Phillips, M. A. *J. Biol. Chem.* **2002**, *277*, 41827.
- Sutton, A. E.; Clardy, J. *Tetrahedron Lett.* **2001**, *42*, 547.
- Knecht, W.; Bergiohann, U.; Gonski, S.; Kirschbaum, B.; Löffler, M. *Eur. J. Biochem.* **1996**, *240*, 292.
- Otwinowski, Z.; Minor, W. *Methods Enzymol.* **1997**, *276*, 307.
- Collaborative Computational Project, N. *Acta Crystallogr. D Biol. Crystallogr.* **1994**, *50*, 760.
- Jones, T. A.; Zou, J. Y.; Cowan, S. W.; Kjeldgaard, M. *Acta Crystallogr. A* **1991**, *47*, 110.
- Kleywegt, G. J.; Jones, T. A. *Acta Crystallogr. D Biol. Crystallogr.* **1996**, *52*, 829.
- Brünger, A. T.; Adams, P. D.; Clore, G. M.; DeLano, W. L.; Gros, P.; Grosse-Kunstleve, R. W.; Jiang, J.-S.; Kuszewski, J.; Nilges, M.; Pannu, N. S.; Read, R. J.; Rice, L. M.; Simonson, T.; Warren, G. L. *Acta Crystallogr. D Biol. Crystallogr.* **1998**, *54*, 905.
- Kleywegt, G. J.; Jones, T. A. *Acta Crystallogr. D Biol. Crystallogr.* **1998**, *54*, 1119.
- Christopher, J. A. *SPOCK: The Structural Properties Observation and Calculation Kit*, The Center for Macromolecular Design, Texas A&M University: College Station, TX, 1998.
- Kraulis, P. J. *J. Appl. Crystallogr.* **1991**, *24*, 946.
- Fenn, T. D.; Ringe, D.; Petsko, G. A. *J. Appl. Crystallogr.* **2003**, *36*, 944.
- Team, T. P.-R. *POV-Ray—the Persistence of Vision Raytracer*, 3.5x; 2003.
- Kabsch, W.; Sander, C. *Biopolymers* **1983**, *22*, 2577.
- Frishman, D.; Argos, P. *Proteins* **1995**, *23*, 566.
- McLean, J. E.; Neidhardt, E. A.; Grossman, T. H.; Hedstrom, L. *Biochemistry* **2001**, *40*, 2194.
- Bruneau, J. M.; Yea, C. M.; Spinella-Jaegle, S.; Fudali, C.; Woodward, K.; Robson, P. A.; Sautes, C.; Westwood, R.; Kuo, E. A.; Williamson, R. A.; Ruuth, E. *Biochem. J.* **1998**, *336*, 299.
- Chen, S. F.; Ruben, R. L.; Dexter, D. L. *Cancer Res.* **1986**, *46*, 5014.
- Chen, S. F.; Papp, L. M.; Ardecky, R. J.; Rao, G. V.; Hesson, D. P.; Forbes, M.; Dexter, D. L. *Biochem. Pharmacol.* **1990**, *40*, 709.
- Cleaveland, E. S.; Zaharevitz, D. W.; Kelley, J. A.; Paull, K.; Cooney, D. A.; Ford, H., Jr. *Biochem. Biophys. Res. Commun.* **1996**, *223*, 654.
- Knecht, W.; Henseling, J.; Löffler, M. *Chemico-Biol. Interact.* **2000**, *124*, 61.
- Lakaschus, G.; Löffler, M. *Biochem. Pharmacol.* **1992**, *43*, 1025.
- Peters, G. J.; Sharma, S. L.; Laurensse, E.; Pinedo, H. M. *Investig. New Drugs* **1987**, *5*, 235.
- Knecht, W.; Löffler, M. *Adv. Exp. Med. Biol.* **2000**, *486*, 267.
- Seymour, K. K.; Lyons, S. D.; Phillips, L.; Rieckmann, K. H.; Christopherson, R. I. *Biochemistry* **1994**, *33*, 5268.
- Kobayashi, K.; Nakashima, A.; Nagata, H.; Nakajima, H.; Yamaguchi, K.; Sato, S.; Miki, I. *Inflamm. Res.* **2001**, *50*, 24.
- Bennett, L. L., Jr.; Smithers, D.; Rose, L. M.; Adamson, D. J.; Thomas, H. J. *Cancer Res.* **1979**, *39*, 4868.
- Cleaveland, E. S.; Monks, A.; Vaigro-Wolff, A.; Zaharevitz, D. W.; Paull, K.; Ardalán, K.; Cooney, D. A.; Ford, H., Jr. *Biochem. Pharmacol.* **1995**, *49*, 947.
- Jaffee, B. D.; Jones, E. A.; Loveless, S. E.; Chen, S. F. *Transplant. Proc.* **1993**, *25*(3 Suppl. 2), 19.
- Williamson, R. A.; Yea, C. M.; Robson, P. A.; Curnock, A. P.; Gadher, S.; Hambleton, A. B.; Woodward, K.;

- Bruneau, J. M.; Hambleton, P.; Moss, D., et al. *J. Biol. Chem.* **1995**, *270*, 22467.
53. Williamson, R. A.; Yea, C. M.; Robson, P. A.; Curnock, A. P.; Gadher, S.; Hambleton, A. B.; Woodward, K.; Bruneau, J. M.; Hambleton, P.; Spinella-Jaegle, S.; Morand, P.; Courtin, O.; Sautes, C.; Westwood, R.; Hercend, T.; Kuo, E. A.; Ruuth, E. *Transplant. Proc.* **1996**, *28*, 3088.
54. Hudson, A. T.. In Leeming, P. R., Ed.; *Topics in Medicinal Chemistry*; Royal Society of Chemistry: London, England, 1988; Vol. 65, p 367.
55. Leban, J.; Saeb, W.; Garcia, G.; Baumgartner, R.; Kramer, B. *Bioorg. Med. Chem. Lett.* **2004**, *14*, 55.
56. Batt, D. G.; Copeland, R. A.; Dowling, R. L.; Gardner, T. L.; Jones, E. A.; Orwat, M. J.; Pinto, D. J.; Pitts, W. J.; Magolda, R. L.; Jaffee, B. D. *Bioorg. Med. Chem. Lett.* **1995**, *5*, 1549.
57. Batt, D. G.; Petraitis, J. J.; Sherk, S. R.; Copeland, R. A.; Dowling, R. L.; Taylor, T. L.; Jones, E. A.; Magolda, R. L.; Jaffee, B. D. *Bioorg. Med. Chem. Lett.* **1998**, *8*, 1745.
58. Pitts, W. J.; Jetter, J. W.; Pinto, D. J.; Orwat, M. J.; Batt, D. G.; Sherk, S. R.; Petraitis, J. J.; Jacobson, I. C.; Copeland, R. A.; Dowling, R. L.; Jaffee, B. D.; Gardner, T. L.; Jones, E. A.; Magolda, R. L. *Bioorg. Med. Chem. Lett.* **1998**, *8*, 307.
59. Ren, S.; Wu, S. K.; Lien, E. *J. Pharmaceut. Res.* **1998**, *15*, 286.
60. Irwin, J. J.; Shoichet, B. K. *J. Chem. Informat. Model.* **2004**.
61. Zsoldos, Z.; Szabo, I.; Szabo, Z.; Johnson, A. *J. Mol. Struct.: THEOCHEM.* **2003**, *666-667*, 659.
62. Baldwin, J.; Michnoff, C. H.; Malmquist, N. A.; White, J.; Roth, M. G.; Rathod, P. K.; Phillips, M. A. *The Journal of Biological Chemistry.* **2005**, M501100200.;
63. Leban, J.; Kralik, M.; Mies, J.; Baumgartner, R.; Gassen, M.; Tasler, S. *Bioorg. Med. Chem. Lett.* **2005**, *16*, 267.